

## **Legends – Supplemental Online Material**

### **Suppl. Fig. 1 IR-DIC images of synaptically connected L2/3 pyramidal cells and relationship between soma distance and EPSP amplitude.**

A, Low magnification image of an acute thalamocortical slice showing the location of the two recording pipettes in layer 2/3. Here, four barrels in layer 4 (indicated by dashed lines) are clearly visible. Pairs of L2/3 pyramidal cells were located above a barrel (intracolumnar pairs) at distances between 10 and 90  $\mu\text{m}$ .

B, C, High resolution IR-DIC images of a pair of synaptically connected pyramidal cells in layer 2/3; the postsynaptic cell is shown in B and the presynaptic cell in C.

D, Histogram showing the relationship between EPSP amplitude and soma distance of synaptically coupled L2/3 pyramidal cells. Each dot represents an individual synaptic connection. The virtually horizontal regression line indicates that there was no correlation between the two parameters.

### **Suppl. Fig. 2 Time course and amplitude of EPSPs in an individual L2/3 pyramidal cell pair**

Distributions of latency (A), 20-80% rise time (B), decay time constant (C) and EPSP amplitude (D) displaying the variation in these parameters in an individual pair of synaptically connected L2/3 pyramidal cells. The noise distribution is also shown in panel D.

### **Suppl. Fig. 3 EPSCs time course at the L2/3-L2/3 pyramidal cell connection**

A, recording of the mean unitary EPSP (top trace) and mean EPSC (bottom trace) in the same pair of synaptically connected L2/3 pyramidal cells. Note that the rapid EPSC decay contrasts sharply with that of the EPSP. B, histogram of 20-80% EPSC

rise times (mean:  $0.35 \pm 0.16$  ms) and C, decay time constants (single exponential fits to the falling phase; mean:  $3.7 \pm 1.2$  ms).

**Suppl. Fig. 4 Target structures of L2/3 pyramidal cell axons**

A, Camera lucida reconstruction of a L2/3 pyramidal cell with long-range axonal collaterals spanning more 2 mm of cortical surface. The dendritic domain of the L2/3 pyramidal cells is shown in white and its axon in green. Electron microscopic analysis was performed on proximal (marked with ★) and distal (marked with ○) axonal profiles of the L2/3 pyramidal cell.

B, Electron microscopy of synaptic contacts established by horizontal axonal collaterals (indicated by the white asterisk and circle) of the postsynaptic L2/3 pyramidal cell shown in Supplementary Figure 4A on different postsynaptic target structures in layer 2/3 as revealed from serial ultrathin sectioning through the entire axonal domain. Synaptic contacts were established predominantly either on small calibre dendritic shafts (B3, B6, B7) or spines (B1, B4, B5) of excitatory neurones. Synaptic contacts on dendritic profiles of GABAergic interneurons as revealed by GABA postimmunogold-labelling (B2) are rarely found and were established relatively close to the soma of the L2/3 pyramidal cell. Abbreviations: sp, spine; b, biocytin-filled synaptic bouton. Scale bars, 0.5  $\mu$ m.

#### **Methods for Suppl. Fig. 4**

***GABA postembedding immunogold labelling.*** The immunogold staining procedure was carried out as described by Somogyi and Hodgson (1985), using a commercially available antiserum against GABA (Sigma, Munich, Germany). The immunostaining was performed with droplets of Millipore-filtered solutions in humid Petri dishes. Immersion in 1% periodate (10 min) was followed by several washes of bi-distilled water. Thereafter, the grids were transferred through 2 or 5% sodium metaperiodate (10-30 min) and rinsed several times in bi-distilled water and three times in Tris-buffered saline (TBS, pH 7.4). After pre-incubation in 1% ovalbumin dissolved in TBS (30 min), sections were incubated in rabbit anti-GABA antiserum (1:5000, in 1% normal goat serum in TBS). After rinsing in TBS and 50 mM Tris-buffer (pH 7.4) containing 1% bovine serum and 0.5% Tween 20 (10 min), they were incubated in the secondary antibody (goat anti-rabbit IgG-coated colloidal gold, 10 nm) for 2 hrs (diluted 1:10, in darkness). After rinsing in 2% glutaraldehyde (10 min), the grids were washed again in double-distilled water and stained with uranyl acetate and lead citrate. In control experiments without the primary antibody and sections processed for GABA postimmunogold labelling almost no or only low background labelling was detected, whereas labelling of GABAergic structures exceeded the mean gold particle density of the maximal background staining by at least 4 standard deviations.

#### **Results/Discussion for Suppl. Fig. 4**

***Synaptic contacts of long-range horizontal axonal collaterals.*** To identify the different classes of target neurones of L2/3 pyramidal cells within and across columns serial ultrathin sections through the entire axonal domain of L2/3 pyramidal cells with long axonal collaterals (n=5; Suppl. Fig. 4A) were examined. Of the total number of synaptic boutons investigated (n=154 in layer 2/3), the vast majority of target

structures were non-GABAergic, putative excitatory neurones as revealed by GABA postimmunogold labelling. Synaptic contacts were established with either small calibre dendritic shafts (n=46, 29.9%, Suppl. Fig. 4B3,B6,B7) or spines (n=103, 66.9%, Fig. 4B1,B4,B5) of presumably basal dendrites of other L2/3 pyramidal cells. In addition, synaptic contacts were also established, however to a lesser extent, with small calibre dendrites of GABAergic interneurons (n=5, 3.2%, Suppl. Fig. 4B2). We did not find GABAergic profiles outside the 'home' column that were innervated by biocytin-filled synaptic boutons, suggesting that the long-range horizontal connections terminate preferentially on excitatory neurones, presumably other pyramidal cells in layer 2/3.

Despite the sparse innervation of L2/3 inhibitory interneurone by L2/3 pyramidal cells there are numerous sources that are in a position to drive inhibition in layer 2/3. First, thalamocortical input and intracortical layer 4 input feed-forward excitation may recruit inhibitory interneurons in layer 4, a fraction of which may target L2/3 pyramidal cells (Porter et al., 2001; Sun et al., 2006; Kölbl, Helmstaedter, Feldmeyer; unpublished results). Second, excitatory input from layer 4 may drive L2/3 interneurons (Helmstaedter, Sakmann, Feldmeyer; unpublished results) and also L5 interneurons both of which may have axonal projections onto L2/3 pyramidal cells. Third, inhibition of L2/3 pyramidal cells may also be achieved by L1 interneurons with an axonal domain in layer 2/3 (e.g. Chu et al., 2003). Finally, L2/3 interneurons may be recruited by L2/3 pyramidal cells despite a sparse innervation under the condition that the quantal EPSP amplitude for L2/3 pyramidal cell – L2/3 interneurone connections is large.

## References

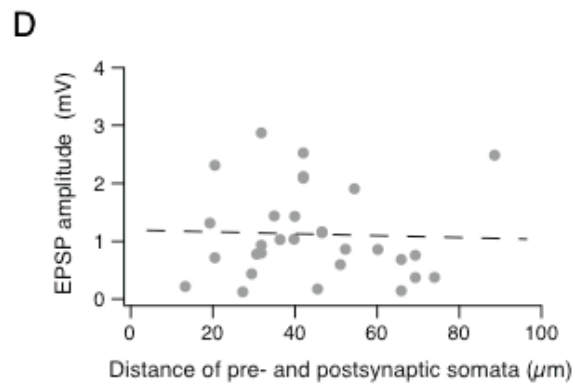
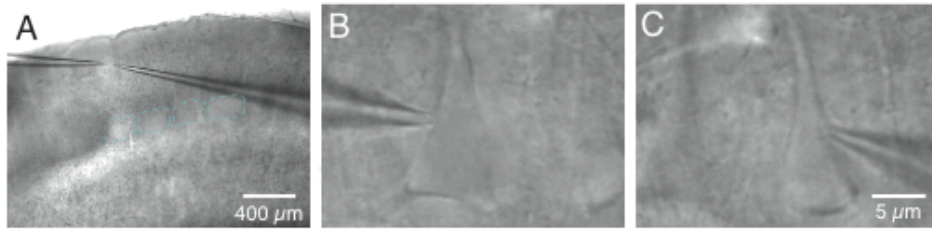
Chu Z, Galarreta M & Hestrin S (2003). Synaptic interactions of late-spiking neocortical neurons in layer 1. *J Neurosci* **23**, 96-102.

Porter JT, Johnson CK & Agmon A (2001). Diverse types of interneurons generate thalamus-evoked feedforward inhibition in the mouse barrel cortex. *J Neurosci* **21**, 2699-2710.

Somogyi, P & Hodgson AJ (1985). Antisera to gamma-aminobutyric acid. III. Demonstration of GABA in Golgi-impregnated neurons and in conventional electron microscopic sections of cat striate cortex. *J Histochem Cytochem* **33**, 249-257.

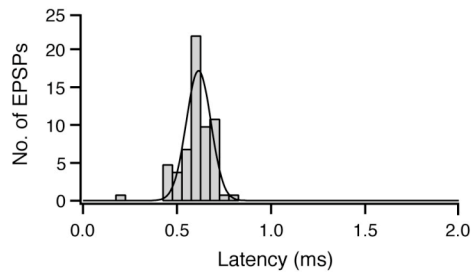
Sun QQ, Huguenard JR & Prince DA (2006). Barrel cortex microcircuits: thalamocortical feedforward inhibition in spiny stellate cells is mediated by a small number of fast-spiking interneurons. *J Neurosci* **26**, 1219-1230.

Suppl. Fig. 1

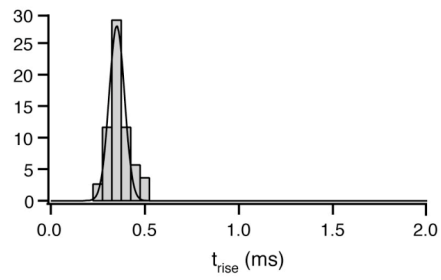


Suppl. Fig. 2

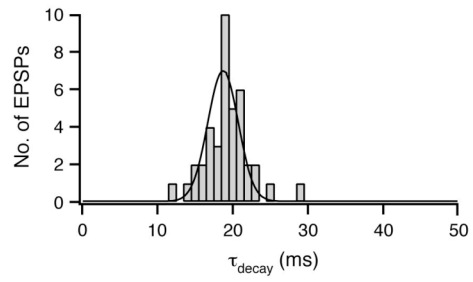
A



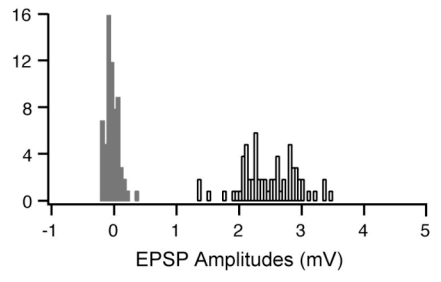
B



C

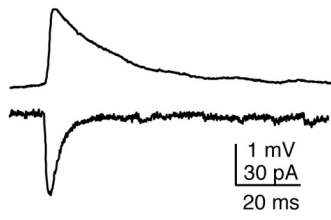


D

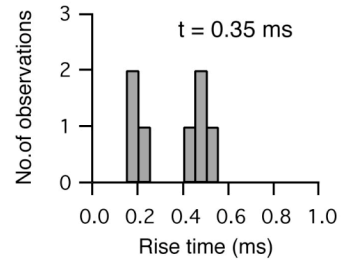


Suppl. Fig. 3

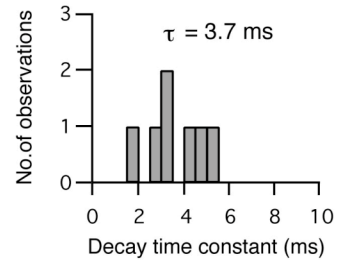
A



B



C





Suppl. Fig. 4

